ISSN 1674-1056
http://cpb.iphy.ac.cn
http://iopscience.iop.org/cpb
中国物理 B
Chinese Physics
中国物理 Chinese Physics B

First-principles study on optic-electronic properties of doped formamidinium lead iodide perovskite

Xin-Feng Diao(刁心峰), Yan-Lin Tang(唐延林), Quan Xie(谢泉)

Citation: Chin. Phys. B . 2019, 28(1): 017802. **doi:** 10.1088/1674-1056/28/1/017802
Journal homepage: http://cpb.iphy.ac.cn; http://iopscience.iop.org/cpb

What follows is a list of articles you may be interested in

Recent research process on perovskite photodetectors:A review for photodetector – materials, physics, and applications

Yan Zhao(赵岩), Chenglong Li(李成龙), Liang Shen(沈亮)
Chin. Phys. B . 2018, 27(12): 127806. **doi:** 10.1088/1674-1056/27/12/127806

Electron transport properties of TiO_2 shell on Al_2O_3 core in dye-sensitized solar cells

Dongmei Xie(解东梅), Xiaowen Tang(唐小文), Yuan Lin(林原), Pin Ma(马品), Xiaowen Zhou(周晓文)
Chin. Phys. B . 2018, 27(1): 017804. **doi:** 10.1088/1674-1056/27/1/017804

Temperature-dependent photoluminescence of size-tunable ZnAgInSe quaternary quantum dots

Qi Ding(丁琪), Xiao-Song Zhang(张晓松), Lan Li(李岚), Jian-Ping Xu(徐建萍), Ping Zhou(周平), Xiao-Fei Dong(董晓菲), Ming Yan(晏明)
Chin. Phys. B . 2017, 26(6): 067804. **doi:** 10.1088/1674-1056/26/6/067804

Temperature-dependent photoluminescence on organic-inorganicmetal halide perovskite $CH_3NH_3PbI_{3-x}Cl_x$prepared onZnO/FTO substrates using a two-step method

Shiwei Zhuang(庄仕伟), Deqian Xu(徐德前), Jiaxin Xu(徐佳新), Bin Wu(伍斌), Yuantao Zhang(张源涛), Xin Dong(董鑫), Guoxing Li(李国兴), Baolin Zhang(张宝林), Guotong Du(杜国同)
Chin. Phys. B . 2017, 26(1): 017802. **doi:** 10.1088/1674-1056/26/1/017802

Fabrication and temperature-dependent photoluminescence spectra of Zn-Cu-In-S quaternary nanocrystals

Liu Xiao-Juan, Zhang Xiao-Song, Li Lan, Wang Xue-Liang, Yuan Lin-Lin
Chin. Phys. B . 2014, 23(11): 117804. **doi:** 10.1088/1674-1056/23/11/117804

First-principles study on optic-electronic properties of doped formamidinium lead iodide perovskite*

Xin-Feng Diao(刁心峰)[1,2], Yan-Lin Tang(唐延林)[3,†], and Quan Xie(谢泉)[1]

[1] School of Big Data and Information Engineering, Guizhou University, Guiyang 550025, China
[2] School of Physics and Electronic Sciences, Guizhou Normal College, Guiyang 550018, China
[3] School of Physics, Guizhou University, Guiyang 550025, China

(Received 12 October 2018; revised manuscript received 6 November 2018; published online 21 December 2018)

We have discussed the materials of solar cell based on hybrid organic–inorganic halide perovskites with formamidinium ($NH_2CH=NH_2^+$ or FA) lead iodide. Firstly, we build the structure of formamidinium lead iodide ($FAPbI_3$) by using the material studio. By using the first-principles calculations, the energy band structure, density of states (DOS), and partial DOS (PDOS) of the hydrazine-iodide lead halide are obtained. Then, we theoretically analyze a design scheme for perovskite solar cell materials, published in [*Science* **354**, 861 (2016)], with the photoelectric conversion efficiency that can reach 20.3%. Also, we use non-toxic elements to replace lead in $FAPbI_3$ without affecting its photoelectric conversion efficiency. Here in this work, we explore the energy band structure, lattice constant, light absorption efficiency, etc. After the Ca, Zn, Ge Sr, Sn, and Ta atoms replacing lead (Pb) and through comparing the spectral distributions of the solar spectrum, it can be found that $FAGeI_3$, $FASnI_3$, and $FAZnI_3$ have better absorbance characteristics in the solar spectrum range. If the band gap structure is taken into account, $FAGeI_3$ will become an ideal material to replace $FAPbI_3$, although its performance is slightly lower than that of $FAPbI_3$. The toxicity of Pb is taken into account, and the Ge element can be used as a substitute element for Pb. Furthermore, we explore one of the perovskite materials, i.e., $FA_{0.75}Cs_{0.25}Sn_{0.25}Ge_{0.75}I_3$ whose photovoltaic properties are close to those of $FA_{0.75}Cs_{0.25}Sn_{0.5}Pb_{0.5}I_3$, but the former does not contain toxic atoms. Our results pave the way for further investigating the applications of these materials in relevant technologies.

Keywords: perovskite, band structure, optic-electronic properties, solar cell

PACS: 78.56.–a, 81.05.Fb, 42.50.Nn **DOI:** 10.1088/1674-1056/28/1/017802

1. Introduction

The limited supply of fossil fuels is bound to come to an end, and using solar cells to turn the energy of sunlight into electricity is expected to become a main renewable energy source.[1–3] In the first generation of solar cells, single crystal silicon was used as the main raw material.[4] The disadvantage is that the consumption of silicon material is large, the production cost is high, the conversion efficiency is close to the theoretical limit, and the room for further development is limited. The second-generation solar cells are mainly based on thin-film solar cells, which greatly reduce production costs and save silicon material.[5–8] Large-area panels can also be made if needed, but the conversion efficiency is low and the stability is poor.

The dye-sensitized tandem solar cells, as third-generation solar cells, have the advantages of simple production process and abundant source of battery materials. Therefore, they can be a trend for future development.[9–13] Since the first application in 2009, perovskite solar cells (PSCs) have developed rapidly in just a few years.[14] Up to now, the reported power conversion efficiency (PCE) of the perovskite-based solar cells is over 20%.[15,16] Designated as perovskite is a material that has a general structure of ABX_3, where A and B are two cations and X is an anion that bonds to both.[17] Koliogiorgos *et al.*[18] discussed the hybrid halide perovskites $MABX_3$ (MA = methylammonium) replaced by $MAGeCl_3$ and $MAGeBr_3$; reference[19] reported that the Sr replacement for Pb in $MAPbI_3$ leads to an energy gap doubling the initial one and thus cannot serve as photovoltaic (PV) applications, and they expected to find lead-free perovskites that can be used in energy technology such as solar cells and optoelectronics. Metal halide perovskites $FAPbX_3$ (FA = formamidinium) possess an efficiency of 20.3% for solar cells.[20] And $FAPbI_3$ has aroused intensive interest in its diverse optoelectronic applications. However, there is no research on the analysis of its working mechanism based on the band theory and spectral absorption theory. Here in this work, we calculate the energy band structure, density of states (DOS), and partial DOS (PDOS) of the hydrazine-iodide lead halide by the first-principles. Then, we theoretically analyze a design scheme for perovskite solar cell materials, published in Ref. [20], with

*Project supported by the National Natural Science Foundation of China (Grant No. 11164004), the Industrial Research Project of Guizhou Province, China (Grant No. GY[2012]3060), the Project of Education Department of Guizhou Province, China (Grant No. [2016]215), and the Special Laboratory Fund of Education Department of Guizhou Province, China (Grant No. GY[2014]217).

†Corresponding author. E-mail: tylgzu@163.com

© 2019 Chinese Physical Society and IOP Publishing Ltd

the photoelectric conversion efficiency that can reach 20.3%, and explore the energy band structure, lattice constant, light absorption efficiency, etc., after the Ca, Zn, Ge Sr, Sn, and Ta atoms have replaced lead. The relevant factors affecting the photoelectric conversion efficiency are analyzed, and also we use non-toxic elements to replace lead in $FAPbI_3$ without affecting its photoelectric conversion efficiency.

2. Results and discussion

The calculations are performed within the framework of the density functional theory (DFT). With this theory we investigate $FAPbI_3$ structure crystal of the organic–inorganic perovskites and the doping crystal of it. The band structure and optical properties are calculated with the cambridge sequential total energy package (CASTEP)[21] code using the Perdew–Burke–Ernzerh of (PBE) version of the generalized gradient approximation (GGA).[22] The exchange–correlation functional is norm conserving pseudopotential with a cutoff energy of 310 eV. All the geometries of the unit cell of these materials with ultrasoft pseudopotentials and the atomic positions and lattice parameters are relaxed until atomic forces are converged to a value smaller than 10^{-5} eV/atom. We build the $FAPbI_3$ crystal structure and obtain the energy band structure, DOS, and PDOS of it; then we replace the Pb atom with Ca, Zn, Ge, Sr, Sn, and Ta atoms separately, and use the functional hybrid HSE06 to obtain its reflection spectrum and absorption spectrum.

Also, we build the doped supercells with $2\times2\times1$ mesh for $FA_{0.75}Cs_{0.25}Sn_{0.5}Pb_{0.5}I_3$ cells, and $3\times2\times1$ mesh for $FA_{0.83}Cs_{0.17}Pb(I_{0.5}Br_{0.5})_3$ cells. The plane-wave cutoff energy for wave function is taken to be 310 eV. The Gaussian smearing is well optimized under sufficient convergence criterion (0.05 eV/Å) for all the calculations. With the above calculation results, we can analyze the mechanism of achieving a very high photoelectric conversion efficiency for $FA_{0.75}Cs_{0.25}Sn_{0.5}Pb_{0.5}I_3$ and $FA_{0.75}Cs_{0.25}Sn_{0.25}Ge_{0.75}I_3$.

2.1. Model of $FAPbI_3$

Recently, many researchers[23–27] have paid attention to the cubic structure model for $FAPbI_3$ with space group symmetry, and they uses this structure of perovskite material to increase the photoelectric conversion efficiency of solar cells by 22%. In Ref. [28], a variety of lattice constants and energy band gaps of $MAGeCl_3$ and $MAGeBr_3$ were reported, the mixed hybrid halide perovskites were discussed, and the values of the energy gap were obtained although no simplified pattern exists. The formamidinium lead iodide ($FAPbI_3$) has the potential to achieve higher performance than the established perovskite solar cells like methylammonium lead iodide ($MAPbI_3$),[27] while maintaining a higher stability. In this work, we focus on the cubic $FAPbI_3$,[29] and the hybrid halide perovskites crystallized into a cubic structure are shown in Fig. 1.

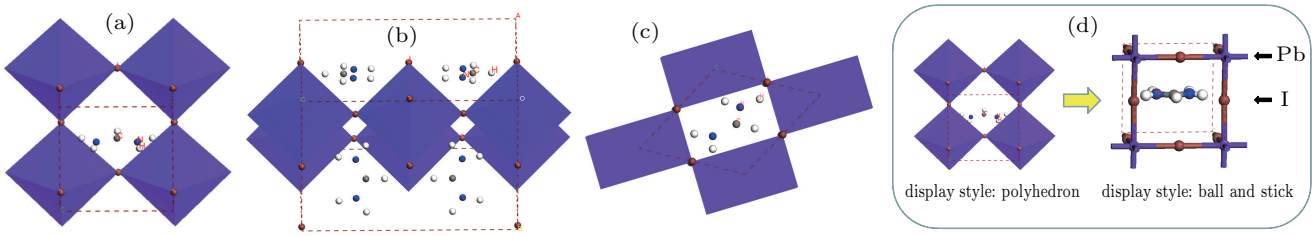


Fig. 1. Crystal structures of perovskite. Since the formamidinium lead iodide perovskite crystal of cubic structure system is widely used, this paper explores the properties of perovskite cubic crystal. The divalent cations sit at the corners of the cube surrounded by halogen atoms in an octahedral environment. The FA cation sits in the center of the cube. (a) Cubic structure, (b) tetragonal structure, (c) orthogonal structure, and (d) comparison of crystal structure.

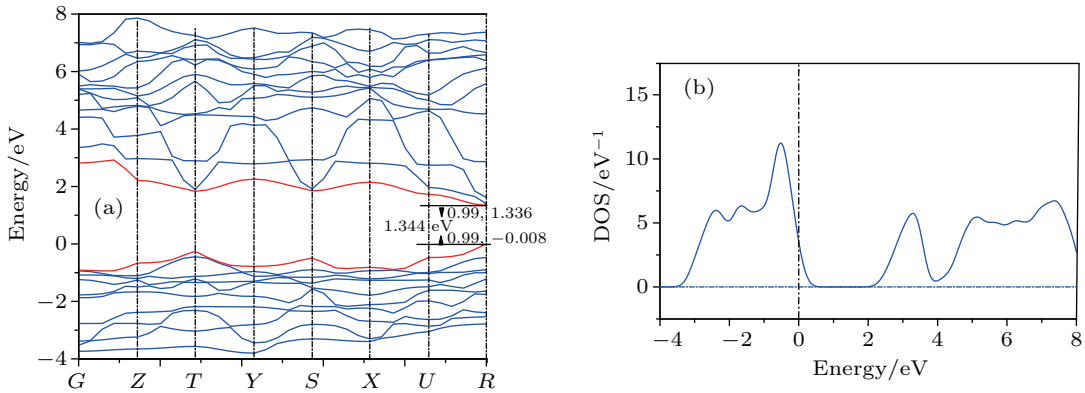


Fig. 2. (a) Band structure and (b) DOS of $FAPbI_3$. The band gap is 1.344 eV.

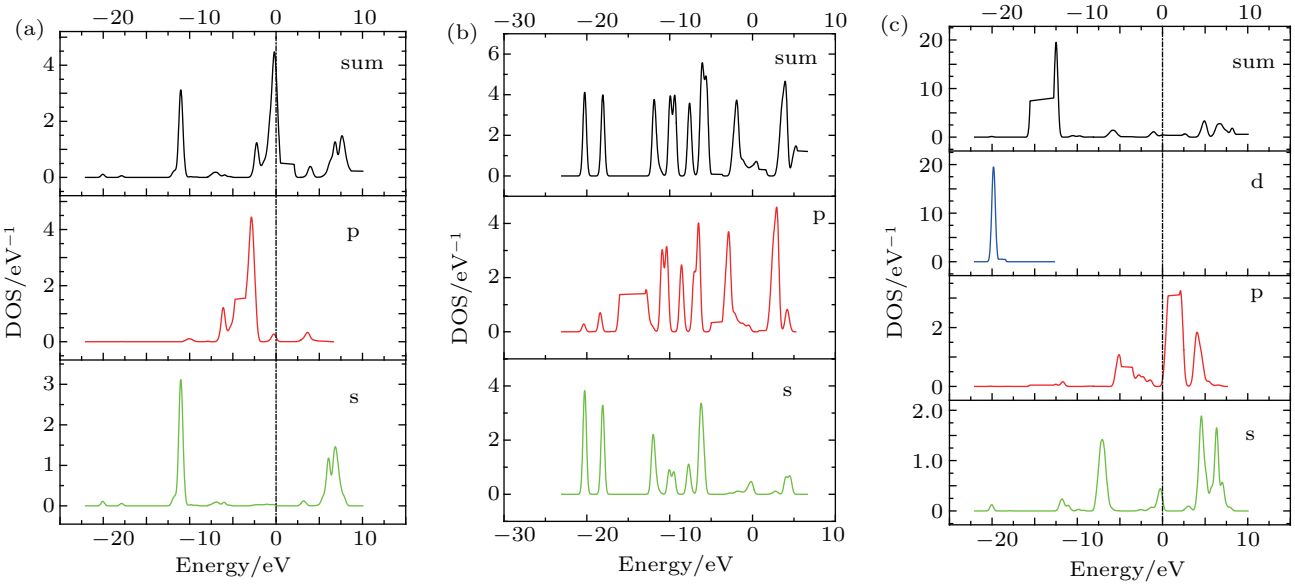


Fig. 3. PDOS of (a) I, (b) FA, and (c) Pb.

We create the cubic $FAPbI_3$ model based on the previously reported results[20] with the crystal of $FAPbI_3$ that has $a = 6.41$ Å, $b = 6.34$ Å, $c = 6.26$ Å, $\alpha = 90°$, $\beta = 90°$, $\gamma = 89.9°$, and the space group of *Pmm*2. The atomic position of the FA cation within this cubic framework is confirmed by total energy calculations. As shown in Fig. 2, the band gap and DOS of $FAPbI_3$ are calculated by the GGA method, presenting an underestimation relating to the available experimental value 1.344 eV, which is in agreement with the result in Ref. [29]. And its corresponding absorption edge reaches 923 nm, which is superior to that of $MAPbI_3$ (1.59 eV) in the sense of serving as a light harvester.

The constituent elements and groups are FA, Pb, and I. We analyze their PDOS, as shown in Fig. 3, which contributes to the DOS that contributes to the s and p electrons of iodine, and s, p, and d electrons of lead atoms. The covalent bond of FA is strong, and the electron density of I exceeds the Fermi level, showing that the metallity is stronger. Because lead is a metal, its s and p orbital electrons all cross the Fermi level, which conforms to reality. It can also be seen that the FA group has a greater influence on the energy band distribution of the perovskite.

In this subsection, we also construct the approximate area of the solar spectrum[30] and introduce the calculated absorption spectra in the same coordinate system. From the point of view of the light absorption spectrum, it can be seen from Fig. 4 that most of the absorption peaks are very few distributed in the visible region when the crystal $FAPbI_3$ is undoped. Most of them are distributed in ultraviolet and other areas.

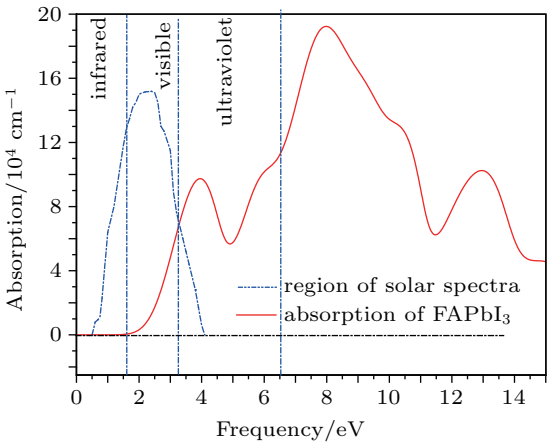


Fig. 4. Optical absorption spectrum of $FAPbI_3$.

2.2. Mixed halide perovskites

In order to study the effect of crystal doping on its photoelectric conversion performance, we build a supercell crystal with $2\times2\times1$ mesh in this subsection. And then we discuss $FAPbI_3$ where FA is replaced with Cs atom at 25%, 50%, 75%, and 100%, and obtain the band gap and its absorption. The crystal structure of $FA_{0.75}Cs_{0.25}PbI_3$ is shown in Fig. 5.

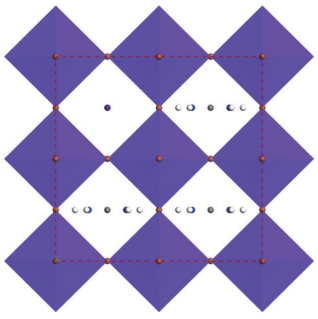


Fig. 5. Model of $FA_{0.75}Cs_{0.25}PbI_3$.

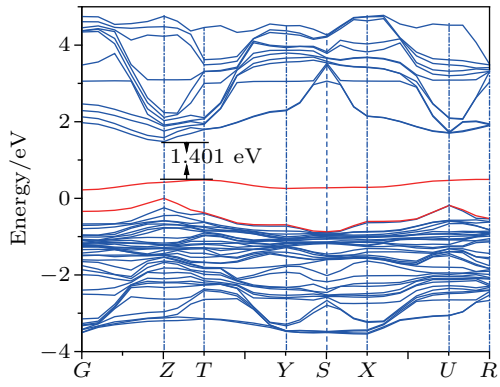


Fig. 6. Band structure of $FA_{0.75}Cs_{0.25}PbI_3$. The band gap is 1.401 eV.

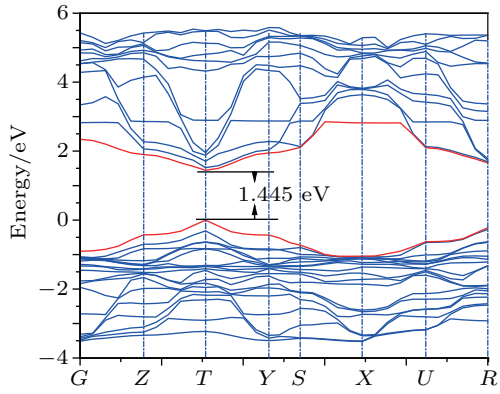


Fig. 7. Band structure of $FA_{0.5}Cs_{0.5}PbI_3$. The band gap is 1.445 eV.

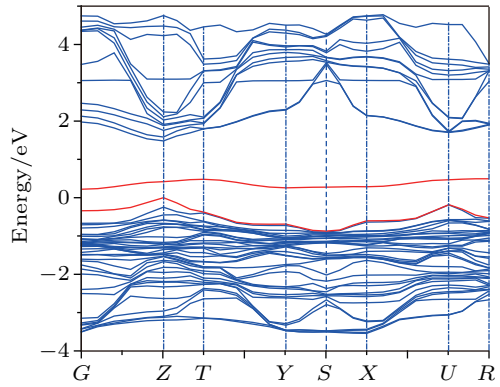


Fig. 8. Band structure of $FA_{0.25}Cs_{0.75}PbI_3$. The band gap is 0.219 eV.

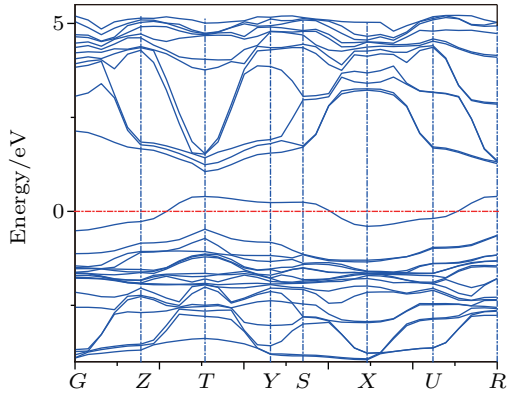


Fig. 9. Band structure of $CsPbI_3$. The band gap is 0.

Comparing the band structure and optical absorption spectra of Figs. 6–10, we find that as the doping ratio increases, the bandgap first increases, and when the ratio exceeds 50%, the bandgap becomes significantly smaller. When the doping is 100%, it shows a distinct metal property. One of the spectral lines spans the Fermi level due to doping atoms. We know that the light radiated from the sun to the earth surface accounts for about 50% in the visible light region, and about 43% in the infrared light region and the ultraviolet light region. Although the band gap is 1.344 eV, theoretically it can absorb the sunlight at wavelengths less than 923 nm. According to the spectral distribution of sunlight radiation to the earth surface, solar cell light-sensitive material hardly covers the visible light and infrared light regions. The band structure and absorption spectrum properties of the doped perovskite material $FAPbI_3$ are ideal for light absorption when the doping Cs structure is 25%.

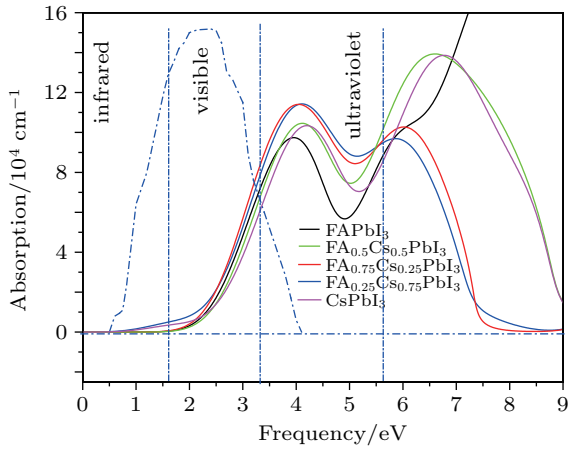


Fig. 10. Optical absorption spectra of various crystal $FA_zCs_{1-z}PbI_3$.

2.3. Theoretical analysis of design scheme for perovskite

Eperon and Leijtens[20] made mechanically stacked four-terminal tandem cells and obtained an efficiency of 20.3% with the materials of $FA_{0.75}Cs_{0.25}Sn_{0.5}Pb_{0.5}I_3$ and $FA_{0.83}Cs_{0.17}Pb(I_{0.5}Br_{0.5})_3$. They discussed the $FA_{0.75}Cs_{0.25}Sn_{0.5}Pb_{0.5}I_3$ that can deliver an efficiency of 14.8%. By combining this material with a wider-band gap $FA_{0.83}Cs_{0.17}Pb(I_{0.5}Br_{0.5})_3$ material, they achieved a monolithic two-terminal tandem efficiency of 17.0% with > 1.65 V open-circuit voltage. However, there is no relevant research on the photoelectric conversion working mechanism from the perspective of density functional theory. Therefore, we use the first-principles calculations to explore the relevant properties of these two structures. The structure models are shown in Figs. 11 and 12.

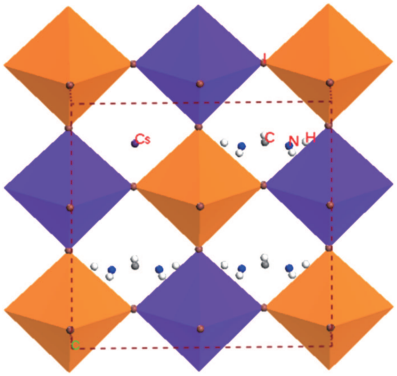


Fig. 11. Structure of $FA_{0.75}Cs_{0.25}Sn_{0.5}Pb_{0.5}I_3$.

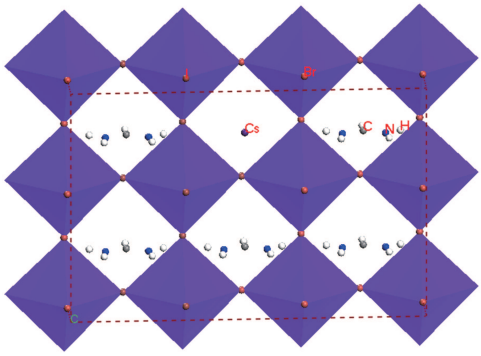


Fig. 12. Structure of $FA_{0.83}Cs_{0.17}Pb(I_{0.5}Br_{0.5})_3$.

Table 1. Band gaps of various crystals of $FA_xCs_{1-x}Sn_{0.5}Pb_{0.5}I_3$ and $FA_{0.75}Cs_{0.25}Sn_{1-y}Pb_yI_3$.

$FA_xCs_{1-x}Sn_{0.5}Pb_{0.5}I_3$						$FA_{0.75}Cs_{0.25}Sn_{1-y}Pb_yI_3$				
Value of x	1	0.25	0.5	0.75	0	Value of y	0	0.5	0.75	1
Band gap/eV	0.806	0.877	0.907	1.003	0.862	Band gap/eV	0.642	1.003	1.122	1.401
Wavelength/nm	1538	1413	1367	1236	1438	Wavelength/nm	1931	1236	1105	885

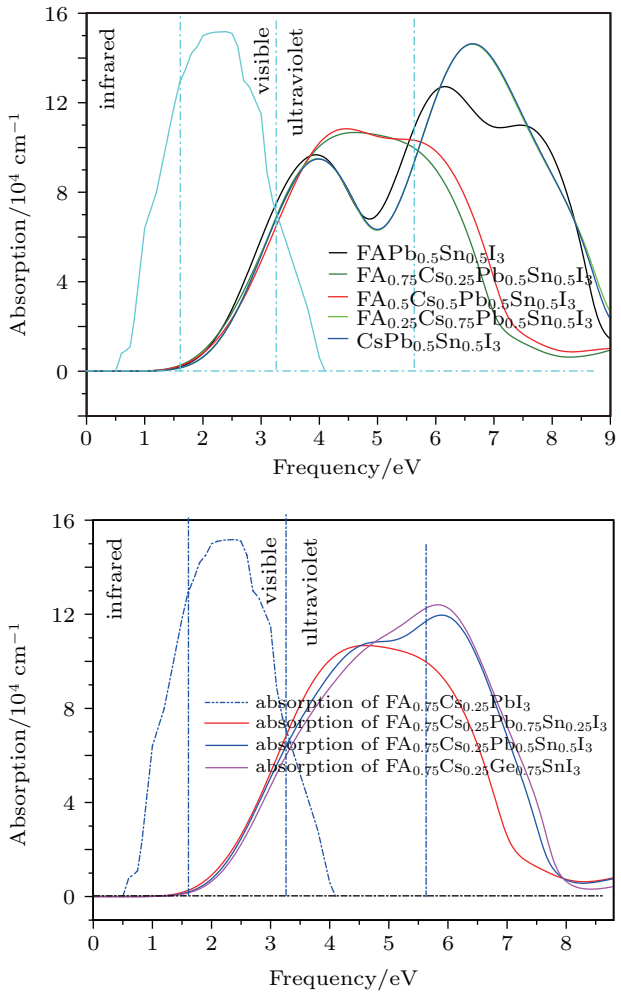


Fig. 13. Optical absorption spectra of $FA_xCs_{1-x}Sn_{0.5}Pb_{0.5}I_3$ and $FA_{0.75}Cs_{0.25}Sn_{1-y}Pb_yI_3$.

We use the controlled variable method to study the effect of doping on crystal band structure and absorption spectrum. After doping Cs and Sn according to Ref. [20], the crystal structures are of $FA_xCs_{1-x}Sn_{0.5}Pb_{0.5}I_3$ and $FA_{0.75}Cs_{0.25}Sn_{1-y}Pb_yI_3$. Using first-principles calculations, the energy bands of various crystals are given in Table 1. According to the relevant quantum mechanics theory, the electrons absorbing the photons to achieve energy level transition must comply with the selection rules in quantum mechanics, i.e., $h\nu \geq E_g$; the absorption wavelength of the solar light can reach 1238 nm. The absorption spectra of $FA_xCs_{1-x}Sn_{0.5}Pb_{0.5}I_3$ and $FA_{0.75}Cs_{0.25}Sn_{1-y}Pb_yI_3$ are shown in Fig. 13. Comparison of the absorption lines of various doped crystal structures shows that both the band gap structure and the light absorption performance of $FA_{0.75}Cs_{0.25}Sn_{0.5}Pb_{0.5}I_3$ are better than those of others. So this structure of perovskite material conduces to the increase of the solar photoelectric conversion efficiency. It is worth noting that $FA_{0.75}Cs_{0.25}Sn_{0.25}Pb_{0.75}I_3$ should also be a good photovoltaic material.

To achieve a better understanding of the optic properties of hybrid organic–inorganic halide perovskites with formamidinium lead iodide, we discuss another $FAPbI_3$ doped perovskite material $FA_{0.83}Cs_{0.17}Pb(I_{0.5}Br_{0.5})_3$. Its crystal structure is shown in Fig. 14, and the band gap is 1.987 eV calculated by first principles, which is slightly larger than the bandgap of 1.6 eV given in Ref. [20], where this material was used to coordinate with $FA_{0.75}Cs_{0.25}Sn_{0.5}Pb_{0.5}I_3$ to make the p–i–n structure to obtain a larger open circuit voltage and substantial photocurrent, for it has a large band gap.

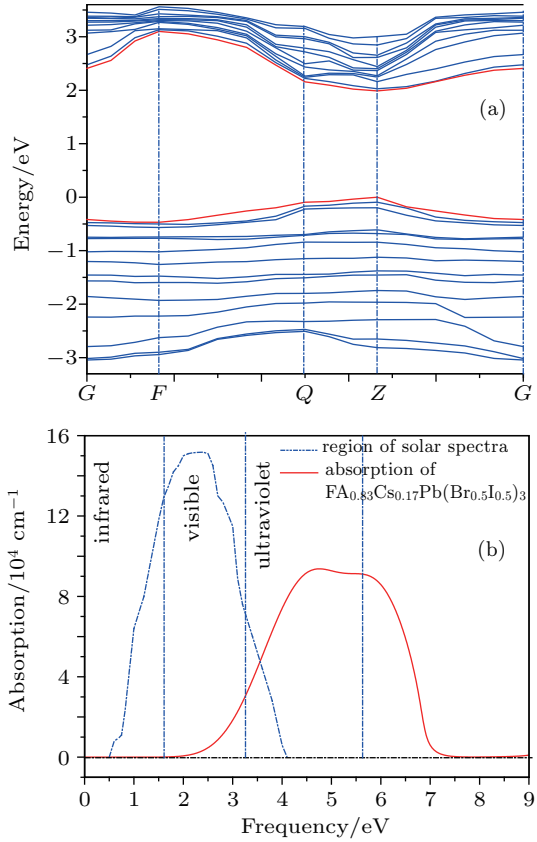


Fig. 14. (a) Band structure and (b) optical absorption spectrum of $FA_{0.83}Cs_{0.17}Pb(I_{0.5}Br_{0.5})_3$. The band gap is 1.987 eV.

2.4. Comparing optical properties of another perovskite

To further explore the effects of doping other non-toxic atoms on their opto–electronic properties, we discuss another $FAPbI_3$ where Pb is replaced separately with the Ca, Zn, Ge, Sr, Sn, and Ta atom, then use ultra-soft pseudo potentials and the valence configuration $1s^1$ for H, $2s^22p^2$ for C, $2s^22p^3$ for N, $5s^25p^5$ for I, and other atoms as shown in Table 1. Further, we get the parameters corresponding to the doping crystal as shown in Table 2 and Fig. 15.

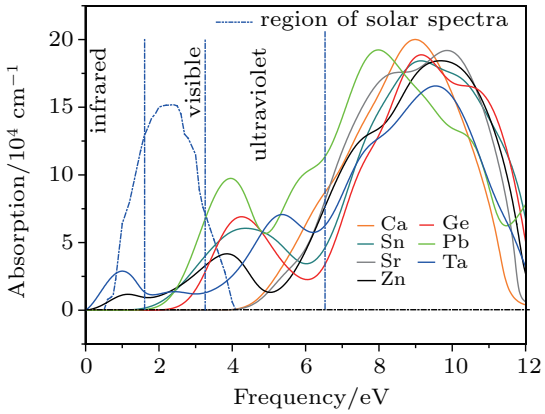


Fig. 15. Absorption spectra of doped materials.

The band gap E_g is the lower limit of the incident spectrum into the battery. A small bandgap width can broaden the absorption of solar light by the battery, but the decrease of E_g makes the concentration index of the intrinsic carrier increase. As a result, the saturated dark current increases greatly and the open circuit voltage decreases. So a small E_g causes the output voltage to decrease, an excessively wide band gap makes the absorption spectrum narrower, renders the excitation of carriers lower, and reduces the photocurrent. Thus, the bandgap that is too wide or too narrow will cause the efficiency to drop. References [31] and [32] show that the bandgap width is in a range of 1.1–1.3 eV, which is an index of good sensitizing dye solar material. By analyzing the data in Table 2 and Fig. 15, we find that $FAGeI_3$ possesses the best optoelectronic performance and a band gap of 1.426 eV that is slightly larger than that of $FAPbI_3$, and the peak of the absorption spectrum is slightly lower than that of $FAPbI_3$. Comparing with the spectral distribution of the solar spectrum, it can be found that the light conversion efficiency of $FAGeI_3$ is lower than that of $FAPbI_3$, but Pb is toxic. If we consider this factor, the Ge atom can be used as an alternative substance for Pb.

Table 2. Calculation results of various crystal parameters.

	$FACaI_3$	$FAZnI_3$	$FAGeI_3$	$FASrI_3$	$FASnI_3$	$FATaI_3$	$FAPbI_3$
Band gap/eV	4.384	0.371	1.426	4.403	0.441	0	1.344
Final energy/eV	–2709	–2986	–1813	–2551	–1803	–1842	–3379
Valence configuration	$3s^23p^64s^2$	$3d^{10}4s^2$	$4s^24p^2$	$4s^24p^65s^2$	$5s^25p^2$	$5d^36s^2$	$5d^{10}6s^26p^2$
Toxicity	nontoxic	nontoxic	nontoxic	nontoxic	nontoxic	nontoxic	toxic

2.5. Exploring one of non-toxic perovskite materials

In order to use the Ge atom to replace Pb atom and obtain the corresponding perovskite structure, we calculate the energy band and absorption spectra of two Ge-doped perovskite crystals. Then we consider that in the crystal of the material $FA_{0.75}Cs_{0.25}Sn_{0.5}Pb_{0.5}I_3$ structure, the Pb atom is replaced with Ge atom, and the corresponding bandgap structure and absorption spectrum characteristics are calculated, as shown in Figs. 16 and 17.

The result shows that the band gap and absorption spectrum of $FA_{0.75}Cs_{0.25}Sn_{0.25}Ge_{0.75}I_3$ are close to that of $FA_{0.75}Cs_{0.25}Sn_{0.5}Pb_{0.5}I_3$ properties according to the bandgap and the optical absorption spectrum. If experimental conditions are permitted in the future, the structure of these perovskite materials can be experimentally obtained to replace the crystal $FA_{0.75}Cs_{0.25}Sn_{0.5}Pb_{0.5}I_3$.

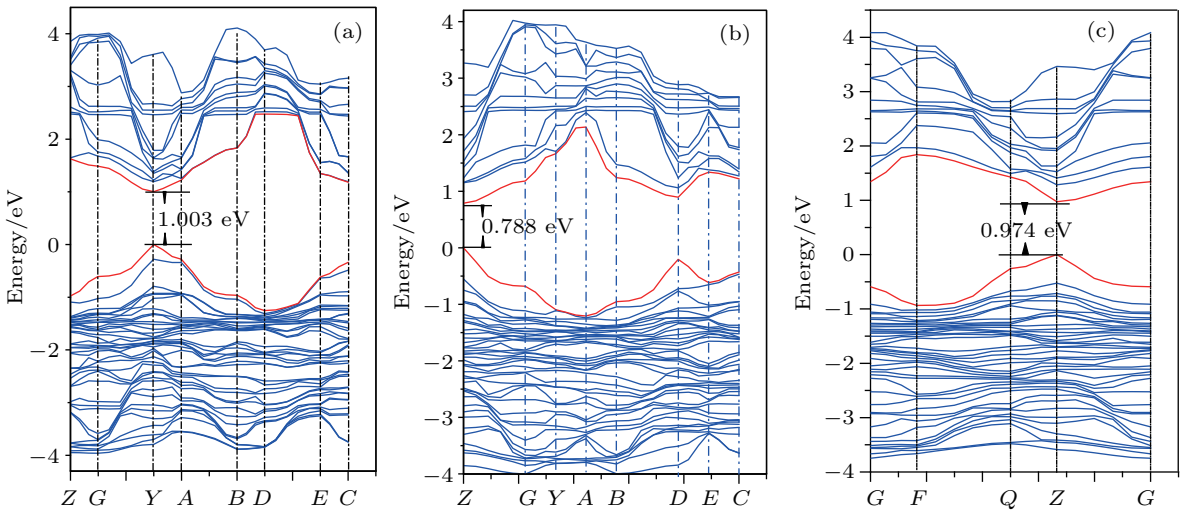


Fig. 16. Band structure of three crystals: (a) $FA_{0.75}Cs_{0.25}Sn_{0.5}Pb_{0.5}I_3$, (b) $FA_{0.75}Cs_{0.25}Sn_{0.5}Ge_{0.5}I_3$, and (c) $FA_{0.75}Cs_{0.25}Sn_{0.25}Ge_{0.75}I_3$. The band gap is (a) 1.003 eV, (b) 0.788 eV, and (c) 0.974 eV.

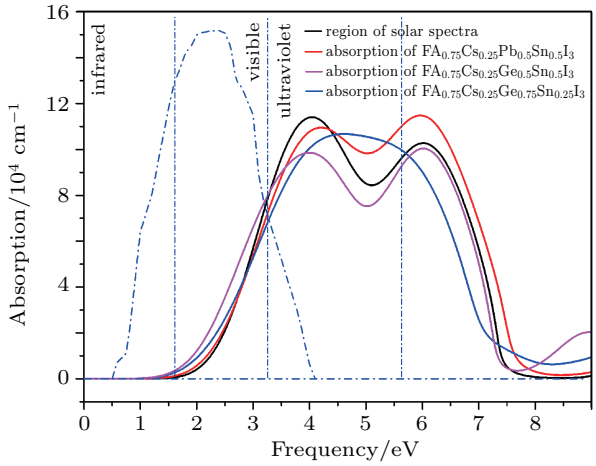


Fig. 17. Optical absorption spectra of three crystals: $FA_{0.75}Cs_{0.25}Sn_{0.5}Pb_{0.5}I_3$, $FA_{0.75}Cs_{0.25}Sn_{0.5}Ge_{0.5}I_3$, and $FA_{0.75}Cs_{0.25}Sn_{0.25}Ge_{0.75}I_3$.

3. Conclusion

In this work, we use the first-principles to calculate the atomic structure and optoelectronics properties of hybrid organic–inorganic halide perovskites with formamidinium lead iodide. To attempt to identify new lead-free halide perovskites, we use CASTEP to obtain the band structure and absorption spectrum curve. Firstly, we study the energy band structure, the PDOS curve, and the absorption spectrum of the $FAPbI_3$. And then, we discuss the lattice doped with C_S atom at 25%, 50%, 75%, and 100%, separately. The result shows that as the doping ratio increases, the band-gap increases; when the doping ratio exceeds 50%, the bandgap becomes significantly smaller. When the doping is 100%, it shows a distinct metal property. From Fig. 9, we can find that one of the spectral lines spans the Fermi level due to doping atoms. A perovskite material with high photoelectric conversion efficiency is reported based on Ref. [20], and we explain the reason for the higher energy absorption band and the band structure.

To further explore the effects of doping other non-toxic atoms on their optoelectronic properties, we discuss the properties of materials obtained by replacing Pb in $FAPbI_3$ with Ca, Zn, Ge, Sr, Sn, and Ta atoms, respectively. The related factors affecting the photoelectric conversion efficiency are analyzed. As is well known, the electrons absorbing the photons to achieve energy level transition must comply with the selection rules in quantum mechanics, i.e., $h\nu \geq E_g$. The wide band gap will result in less absorption of sunlight and low photoelectric conversion efficiency. But if the band gap is too narrow, the carrier kinetic energy generated when absorbing photons with high energy is very large. In this case, downloaded carriers can easily interact with the lattice and then transfer energy to lattice vibration to lose that energy. At the same time, it is easy to form dark current and reduce the photoelectric conversion efficiency. Comparison of the spectral distributions of the solar spectrum shows that $FAGeI_3$, $FASnI_3$, and $FAZnI_3$ have better absorbance characteristics in the solar spectral range. If the band gap structure is taken into account, $FAGeI_3$ will become an ideal material to replace $FAPbI_3$ although its performance is slightly lower than $FAPbI_3$. And considering the toxicity of Pb, the Ge element can be used as an alternative substance for Pb. Moreover, we explore one of the perovskite materials, i.e., $FA_{0.75}Cs_{0.25}Sn_{0.25}Ge_{0.75}I_3$ whose photovoltaic properties are close to those of $FA_{0.75}Cs_{0.25}Sn_{0.5}Pb_{0.5}I_3$, but the former does not contain toxic atoms. Our results pave the way for further investigating the applications of these materials in relevant technologies.

References

[1] Yang L, Barrows A T, Lidzey D G and Wang T 2016 *Rep. Prog. Phys.* **79** 026501

[2] Merabet B, Alamri H, Djermouni M, Zaoui A, Kacimi S, Boukortt A and Bejar M 2017 *Chin. Phys. Lett.* **34** 016101

[3] Xue D J, Shi H J and Tang J 2015 *Acta Phys. Sin.* **64** 038406 (in Chinese)
[4] Andersson B A 2000 *Prog. Photovoltaics* **8** 61
[5] Jiang S, Jia R, Tao K, Hou C X, Sun H C, Yu Z Y and Li Y T 2017 *Chin. Phys. B* **26** 087802
[6] Jackson P, Hariskos D, Wuerz R, Kiowski O, Bauer A, Friedlmeier T M and Powalla M 2015 *Phys. Status Solidi RRL* **9** 28
[7] Burschka J L, Pellet N, Moon S J, Robin H B, Gao P, Nazeeruddin M K and Gratzel M 2013 *Nature* **499** 316
[8] Yang J, Zhao D G, Jiang D S, Liu Z S, Chen P, Li L, Wu L L, Le L C, Li X J, He X G, Wang H, Zhu J J, Zhang S M, Zhang B S and Yang H 2013 *Chin. Phys. B* **22** 098801
[9] Mathew S, Yella A, Gao P, Robin H B, Curchod B F E, Negar A A, Tavernelli I, Rothlisberger U, Nazeeruddin M K and Grätzel M 2014 *Nat. Chem.* **6** 242
[10] Chiang C H, Nazeeruddin M K, Grätzel M and Chun J W 2017 *Energy Environ. Sci.* **10** 808
[11] Lam J Y, Chen J Y, Tsai P C, Hsieh Y T, Chueh C C, Tung S H and Chen W C 2017 *RSC Adv.* **7** 54361
[12] Saliba M, Matsui T, Domansk K, Seo J Y, Ummadisingu A, Zakeeruddin S M, Correa-Baena J P, Tress W R, Abate A, Hagfeldt A and Grätzel M 2016 *Science* **354** 206
[13] Shi B, Guo S, Wei C C, Wei C C, Li B Z Li B, Ding Y, Li Y L, Wan Q, Zhao Y and Zhang X D 2018 *Chin. Phys. B* **27** 018807
[14] Kojima A, Teshima K, Shirai Y and Miyasaka T 2009 *J. Am. Chem. Soc.* **131** 6050
[15] Yang W S, Noh J H, Jeon N J, Kim Y C, Ryu S, Seo J and Seok S I 2015 *Science* **348** 1234
[16] McMeekin D P, Sadoughi G, Rehman W, Eperon G E, Saliba M, Hörantner M T, Haghighirad A, Sakai N, Korte L, Rech B, Johnston M B, Herz L M and Snaith H J 2016 *Science* **351** 151
[17] Pena M A and Fierro J L G 2001 *Chem. Rev.* **101** 1981
[18] Koliogiorgos A, Sotirios B and Galanakis I 2017 *Comput. Mater. Sci.* **138** 92
[19] Jacobsson T J, Pazoki M, Hagfeldt A and Edvinsson T 2015 *J. Phys. Chem. C* **119** 25673
[20] Eperon G E, Leijtens T, Bush K A, *et al.* 2016 *Science* **354** 861
[21] Clark S J, Segall D, Pickard C J, Hasnip P J, Probert M I J, Refson K and Payne M C 2005 *Z. Für Kristallo Graphie* **220** 567
[22] Perdew J P, Wang Y 1992 *Phys. Rev. B* **45** 13244
[23] Jeon N J, Noh J H, Yang W S, Kim Y C, Ryu S, Seo J and Seok S I 2015 *Nature* **517** 476
[24] Han Q, Bae S H, Sun P, Hsieh Y S, Yang Y, Rim Y T, Zhao H X, Chen Q, Shi W Z, Li G and Yang Y 2016 *Adv. Mater.* **28** 2253
[25] Yang W S, Noh J H, Jeon N J, Kim Y C, Ryu S C, Seo J W and Seok S I 2015 *Science* **348** 1234
[26] Pellet N, Gao P, Gregori G, Yang T Y, Nazeeruddin M K, Maier J and Gratzel M 2014 *Angew. Chem. Int. Ed.* **53** 3151
[27] Binek A, Hanusch F C, Docampo P and Bein T 2015 *J. Phys. Chem. Lett.* **6** 1249
[28] Koliogiorgos A, Baskoutas S and Galanakis I 2017 *Comput. Mater. Sci.* **138** 92
[29] Guo Y, Li C B, Li X C, Niu Y S, Hou S G and Wang F 2017 *J. Phys. Chem. C* **121** 12711
[30] Fan Q Y, Chai C C, Wei Q and Yang Y T 2016 *Phys. Chem. Chem. Phys.* **18** 12905
[31] Marinado T, Nonomura K, Nissfolk J, Karlsson D K, Sun L C, Mori S and Hagfeldt A 2010 *Langmuir* **26** 2592
[32] Li W, Bai F Q, Chen J, Wang J and Zhang H X 2015 *Application J. Power Sources* **275** 207